J. Fluid Mech. (1980), *vol.* 101, *part* 4, *pp.* 687–703
Printed in Great Britain

The mixing layer of Loch Ness

By S. A. THORPE AND A. J. HALL

Institute of Oceanographic Sciences, Wormley, Godalming, Surrey, U.K.

(Received 18 February 1980 and in revised form 15 June 1980)

Measurements of the thermal and velocity structure of the near-surface mixing layer of a freshwater lake in moderate wind conditions from fixed or mobile arrays of sensors reveal large-scale coherent structures consisting of narrow fronts across which both the temperature and the horizontal component of the current increase. These fronts are generally transverse to the wind direction and are inclined to the vertical, and appear to be similar to fronts, reported as temperature 'ramps', in the near-surface atmospheric boundary layer. The time derivatives of the temperature are skewed in a sense consistent with observations in laboratory and atmospheric boundary layers, and of a magnitude consistent with measurements in the latter. Evidence is presented to show that bubbles generated by breaking waves are carried down in the large-scale pattern of flow associated with the fronts in the mixing layer. The presence of a Langmuir circulation associated with wind rows has not been established in these experiments. The relevance of the observations to the ocean mixing layer is discussed.

1. Introduction

'Some of the observations ... throw much light on obscure oceanographical problems. Most of the observations could, with advantage, have been carried further, by means of improved instruments ...'. Thus wrote Sir John Murray and Laurence Puller in the preface of the report of the scientific results of the Bathymetrical Survey of the Scottish Fresh-water Lochs during the years 1897–1909 (Murray & Puller 1910). It was in the spirit of these remarks that we began observations in one of the largest freshwater lakes in Scotland, Loch Ness. A review of our early experiments has been published elsewhere (Thorpe 1977). The majority of these experiments were made in the loch thermocline but, with increased confidence in our ability to make accurate measurements and with the development of new instruments, we began an examination of the near-surface mixing layer, which is the subject of this report. (For brevity we shall refer to it simply as the mixing layer.) Following our earlier work we here mean the layer immediately adjoining the surface where the mean gradient Richardson number is small or negative, where a vertical profile of density (or temperature in the freshwater loch; the two are directly related with no salinity effect as in the ocean) is gravitationally unstable over 30 % or more of the region, and where the displacements (as defined by Thorpe 1977) are distributed in nearly Gaussian manner (see also Thorpe 1978*a*). This is a region of active mixing containing small, but (as tracers) significant, temperature fluctuations, isotropic only on scales small compared to the thickness of the layer (Thorpe & Hall 1977),

0022–1120/80/4654–2990 $02.00

although, as we shall show, containing thermal structures which extend in a coherent pattern through a large proportion of the thickness.

Jones & Kenney (1977) suggested a similarity between the mixing layer and the atmospheric boundary layer. They assembled data from several lake and ocean upper layers and showed that their velocity frequency spectra collapsed approximately onto those measured by Bradshaw (1967) in the laboratory, when scaled with shear stress and distance from the surface. The existence of a free upper surface, and in particular the possible effects of surface waves, may however be important. The presence of lines of foam or debris, wind rows, on the surface of lakes or oceans and the associated Langmuir circulation pattern, have attracted much attention. Numerous theories have been offered to explain the appearance of wind rows (see Pollard 1977, for a comprehensive review). Recent work by Garrett (1976), Leibovich (1977) and Leibovich & Radhakrishnan (1977), and laboratory experiments by Faller & Caponi (1978), ascribe their generation to surface-wave interactions (although if this is substantiated, the effects of wind rows will then be absent in boundary-layer flow over a rigid wall, or perhaps replaced by other processes). Whilst, however, Garrett's model predicts that the highest surface waves will be in the convergence zone at the wind row, the theory of Leibovich and his co-authors predicts high waves midway between the rows. Meid (quoted by Pollard) found that the surface wave height was significantly higher, by a factor of about 2, in wind rows than between. This result has not been substantiated by experiments in Loch Ness using a capacitance wire probe (Thorpe & Humphries 1980). At wind speeds of 6·3 (and 8·0) m s^{-1} the significant wave height in wind rows was $39{\cdot}2 \pm 6{\cdot}8$ ($44{\cdot}8 \pm 5{\cdot}0$) cm whilst between it was not significantly different, $39{\cdot}8 \pm 12{\cdot}2$ ($44{\cdot}3 \pm 3{\cdot}2$) cm. The wave periods were $2{\cdot}35 \pm 0{\cdot}13$ ($2{\cdot}51 \pm 0{\cdot}07$) s and $2{\cdot}34 \pm 0{\cdot}09$ ($2{\cdot}42 \pm 0{\cdot}07$) s respectively.† No significant change in the frequency of wave breaking in or between wind rows was found.

Few related observations have been made of the mixing-layer structure and wind rows. The best available seem to be those of Scott *et al.* (1969) who show thermal anomalies extending to 3 m below a wind row (or streak) at low wind speeds. Kenney (1977), in measurements in the shallow Lake of the Woods in Canada, reported that the shear stress spectrum scales with the wind stress and depth, supporting the similarity noticed by Jones & Kenney (1977). The stress-producing eddies had periods of about 10 minutes. Although carefully observing wind rows when making his velocity measurements, Kenney found little evidence to support the hypothesis of a Langmuir pattern of circulation, other than a tendency for particles scattered on the surface to converge towards the streak lines. Thorpe & Stubbs (1979) found no connexion between the depth to which clouds of bubbles caused by breaking surface waves descend and the presence or absence of a wind row. The importance of Langmuir circulation in the mixing layer in comparison with other processes is not clear.

The experiments reported here are in periods in which the loch thermocline is becoming established, that is in the Spring, and during periods later in the year of small or positive heat transfer into the loch. In winds of about 8 m s^{-1} or so, the mixing layer extends to 10–15 m. Our early measurements of the temperature field in the layer (Thorpe & Hall 1977; Thorpe 1978*a*) revealed the existence of narrow

† Here and elsewhere, the $\pm$ value represent one standard deviation unless otherwise specified.

surfaces across which the temperature changed significantly and in which its gradient was high. At a fixed position the advection of the surfaces past a thermistor produces a sudden change in temperature, over distances of as little as 5 cm, very similar to the 'temperature ramps' observed in the atmosphere boundary layer (for references see Antonia *et al.* 1979).

The time, or horizontally, averaged temperature of the mixing layer increases upwards and a rise in temperature is observed as the surfaces, or thermal 'fronts', pass the fixed sensor. Between the 'fronts' the mean temperature gradually falls, although rapid and large fluctuations are present. Observed with two vertically separated thermistors the fronts are found to arrive first at the upper sensor, suggesting that they are either descending through the water column or inclined to the horizontal and advecting horizontally in the flow. The density gradient in the fronts is gravitationally stable with warmer fluid lying above colder. Between the fronts the stratification is more uniform and frequently unstable over vertical scales of a metre or so. It is perhaps significant that the mean horizontal flow and vertical density profiles are (sometimes) found to be marginally unstable to disturbances of wavelength several times the mixing-layer thickness (Thorpe & Hall 1977).

Two questions about the structure of the fronts were raised by these observations: is a thermal front associated with a structure of the flow field, and what is the three-dimensional nature of the surface defining the front? New instruments and arrays were devised to seek answers to these questions, and these are described in §2. Sampling of temperatures and currents was at 1 Hz and, for the advection speeds typical of the Loch, dissipation scales were not sampled.

2. Instruments

2.1. *Moored current and temperature array*

In 1978 a vertical array of seven 'cold' and 'heated' thermistor sensors were deployed on a mooring close to the profiling current meter (P.C.M.) used in earlier experiments to measure vertical profiles of temperature and horizontal current (Thorpe 1977). The seven sensors were spaced at 50 cm intervals, a scale on which thermal fluctuations had earlier been found coherent, on a vertical spar mounted above a Savonious rotor and small direction-finding vane, themselves supported on the upper part of a 3 m tube connected to shore by an 8 core cable. The tube was itself orientated in the flow by a large vane, and was buoyant, supporting a vertical length of the cable which passed from the tube to a sheave fixed in the bottom of the loch at a depth of some 160 m and thence to an electric capstan on shore. The position of the array in the water column could be adjusted by hauling in, or letting out, cable from shore, and was set according to the information obtained from the P.C.M.

Data from each of the seven sensors, the vane, rotor, a pressure sensor on the tube and a compass which determined the tube orientation, were multiplexed down the cable and recorded on magnetic tape at 1 s intervals. In addition a measure of the tilt of the tube was displayed and noted regularly. In the observations described later the tilt was never more than 4°.

The cold thermistors on the sensors are sensitive to temperature whilst the heated thermistors operated at 4 K overheat, are sensitive to both the temperature changes in the surrounding fluid and to current speed. Most of the effect of temperature

change can be compensated for by incorporating a second cold thermistor in the circuitry (see Riedl & Machan 1972; Labarbera & Vogel 1976) and the residual, arranged to be a minimum at the expected operating temperatures in the loch and equivalent at most to a few tenths of a centimetre per second, was removed during computer processing of the data. The three thermistors were mounted in a 10·0 cm long, 2·2 cm diameter Perspex cylinder to provide protection and, approximately, a cosine response to off-axis velocities. The cylinders were mounted horizontally and aligned approximately in the direction of the mean flow by the vane fixed on the tube. Speed calibration of the sensors was made in a towing tank. Over the selected range, 1–30 cm s^{-1}, the r.m.s. noise was less than 0·2 cm s^{-1}. The residual temperature correction was determined by varying the temperature of water pumped through the cylinders at four constant speeds. Frequent *in situ* calibration was made relative to the Savonious rotor by raising and lowering the array in levels of fairly uniform current and recording the outputs of the sensors as each in turn was at a level previously occupied by the rotor. The calibration was made using a least-mean-squares fit of each sensor against the others and against the known rotor calibration. Variations of the calibration during the two months of use in the loch amounted to at most 10 % and appeared to be due to biological growths on the sensors. In operating conditions there was sometimes evidence of regular variations in speed output at periods of 1–9 s, due to small oscillations in the supporting structure, but as the records show (§3) their performance was good enough to define the large-scale current field and its changes.

2.2. *Moored three-dimensional temperature array*

This was used in 1979 and consisted of 11 'cold' thermistors mounted on a 3 × 3 × 3 m cross array supported as before above a rotor, vane and tube, with recording at 1 s intervals. Six of the thermistors were on the vertical spar of the cross at 50 cm intervals (the lower three were actually sensors of the type described in subsection 2.1), three were aligned at 150 cm in the direction of flow, and four were aligned across the flow. (We have counted the thermistor near the centre of the cross three times.)

2.3. *Inverted echo sounder*

Supplementary information was provided in 1979 by an inverted echo sounder (Thorpe & Stubbs 1979) on an 'adjustable depth' mooring. The sounder was used at fixed depth to follow the vertical movements of five acoustic targets, table-tennis balls, attached by 1 m length fishing lines to swivels on a vertical wire supported above the sounder by a streamline float. The targets were drogued with 16 cm diameter plastic flower pots with the bottoms cut out, and carefully made neutrally buoyant by adding weights. In this configuration the drogued targets were found, in laboratory trials, to tow smoothly and directly behind the swivels. The targets are displaced vertically if the flow has a vertical component, and the upward or downward displacement, h, of the targets and fishing line length, l, give the vertical component of current w,

$$w = \frac{uh}{(l^2 - h^2)^{\frac{1}{2}}},$$

where u is the horizontal component of the current. In practice the horizontal

current was estimated from the sensors on the three-dimensional array and the device was used to give estimates of w and, by using several targets, to examine in a qualitative way the variation in patterns of vertical motion (see §3.2).

2.4. *Towed temperature array*

A cabin cruiser was used in 1979 to tow a near-vertical spar supporting 10 thermistors at 60 cm separation. Towing depths ranged from about 2 to 11 m with recording of the thermistors and two pressure sensors every 1 s. Towing speeds of about 0·6 m s^{-1} (typically five times the flow speeds) were used and these, and the location of the cruiser, were determined from an 8 s interval, time-lapse, ciné film taken by a camera on the hillside some 50 m above the site. A second time-lapse camera with telephoto lens was used to record the appearance of the water surface and in particular the presence of wind rows, above the three-dimensional array (§2.2). Wind speeds, humidity and air and water temperatures were recorded regularly.

3. Results

3.1. *Large-scale structures in the temperature and current field*

Figure 1 shows the variation of temperature and current speed with time measured by the seven sensors (§2.1) between 4·0 and 7·0 m. The record is 40 min long. Figure 2 shows the vertical profiles of density and horizontal current measured by the P.C.M. immediately before and after the record. The mixing layer extends down to about 10 m. The mean wind speed 10 m above the water surface was 4·5 m s^{-1} and the air temperature was about 0·8 K below the water surface temperature, the wet bulb being depressed by 0·3 K. The sky was overcast, weather dry but humid. Occasional white capping was observed and bubbles (see Thorpe & Stubbs 1979) penetrated as far as 1·9 m below the surface.

The temperature record (figure 1) shows a fairly typical 'ramp' structure with abrupt and rapid temperature increases occurring at successively lower levels as described in §1. The interval between successive ramps is 200–300 s. In the period 600–1200 s ramps occur only at the upper thermistors. The current record contains more high-frequency structure (see §2.1) but the same pattern of ramps can be seen with an increase in flow accompanying an increased temperature, both suggesting that the fluid immediately following a ramp or thermal front has originated in the faster moving, warmer, near-surface layers. Figure 3 shows the corresponding isotherms and isovels, computed from 9 s running-mean values and plotted on the assumption that both temperature and velocity increase monotonically upwards. There is a similarity in the gross patterns, and several fronts descending in time (e.g. at 350, 1080, 1280, 1600 s) can be seen in both records. The average cross-correlation coefficient of the two records (excluding the first 1200 s of the lower temperature record when the signal was close to the limit of resolution, 0·001 K) was 0·64.

Ten of the fronts were analysed to determine the apparent speed at which the change in speed or temperature passed from the upper to the lower sensor. Dividing this by the mean horizontal current gives a measure of the inclination of the fronts to the horizontal on the Taylor hypothesis that the pattern is frozen and advected with the flow (see §3.2). This angle was estimated to be $39 \pm 11°$ for the temperature

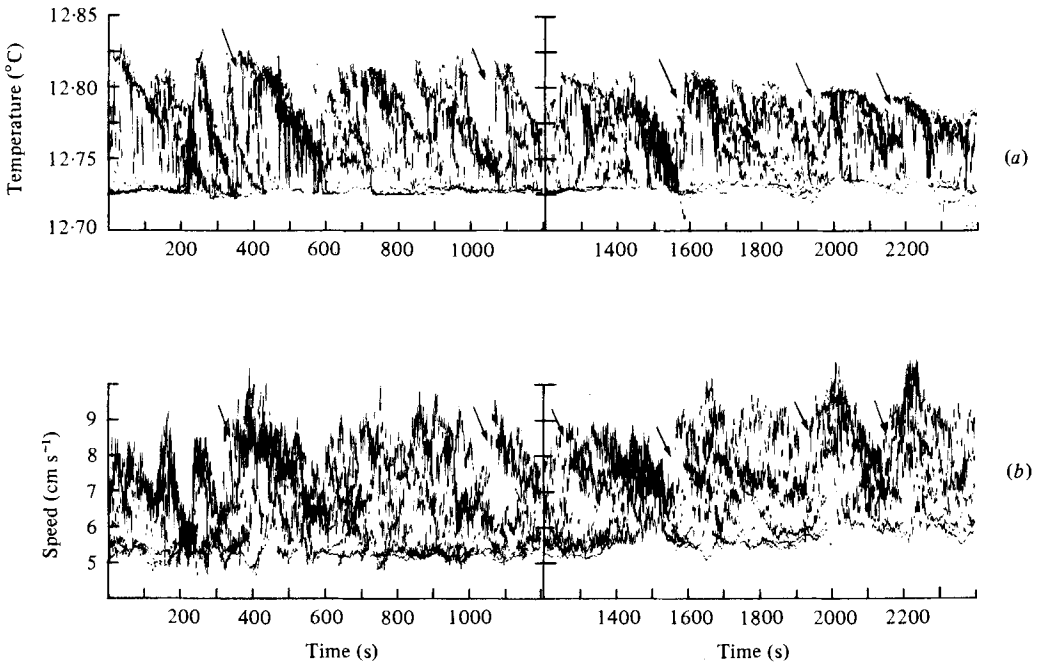

FIGURE 1. (*a*) Temperatures measured by a vertical array of seven thermistors (see § 2.1) extending from 4–7 m depth plotted against time. All seven traces are superimposed. (*b*) The horizontal components of currents in the direction of the mean flow. The arrows draw attention to some of the times when temperature ramps or fronts are passing the sensors, when the currents also increase abruptly.

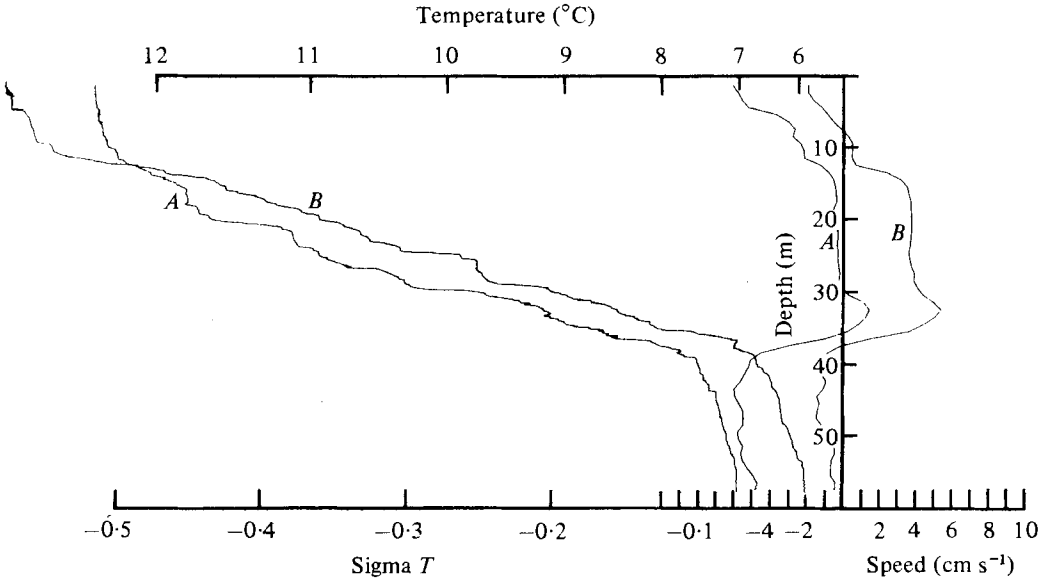

FIGURE 2. Profiles of (to left) temperature and (to right) horizontal current obtained by the P.C.M. before (*A*) and after (*B*) the records of figure 1. The profiles B have been shifted 0·1 sigma T units or 5 cm s^{-1} to the right.

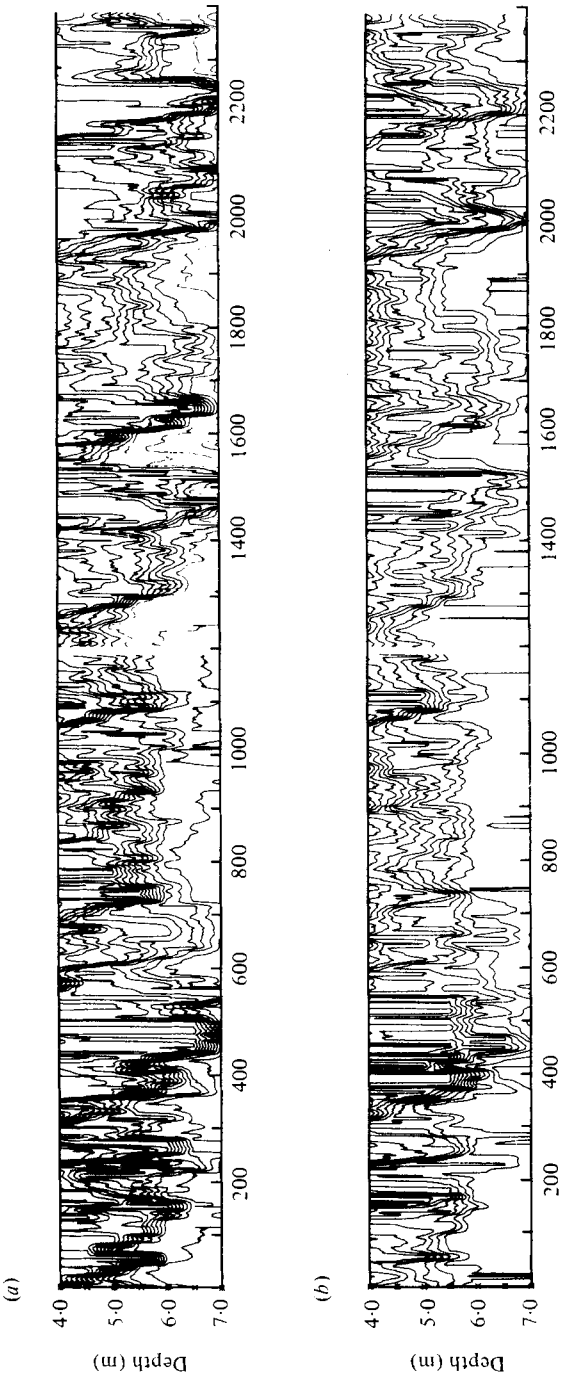

FIGURE 3. (*a*) Isotherms and (*b*) isovels constructed from the data shown in figure 1. Temperatures are contoured at 0·03 K intervals and currents at 0·4 cm s^{-1}.

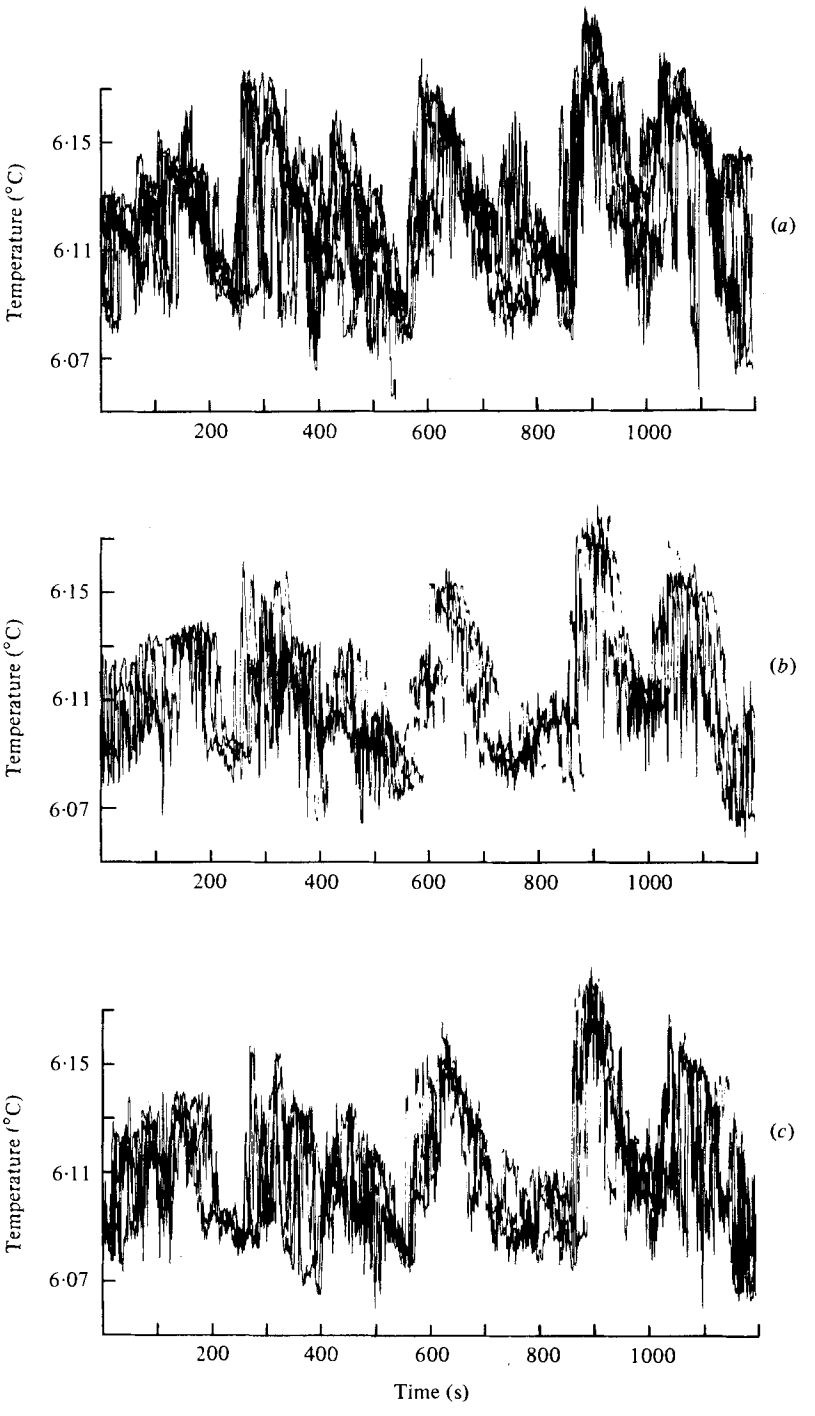

FIGURE 4. Temperature versus time measured by sensors aligned (*a*) in the vertical, (*b*) along the flow direction and (*c*) across the flow direction on the three-dimensional array (§ 2.2). The sensors along and across the flow are at 6·55 m and those in the vertical span the range 4·55–7·05 m.

fronts and $34 \pm 11°$ for the currents. The distance between fronts under the same hypothesis is 13·5–20·2 m. The average gradient Richardson number at the fronts was estimated at 0·15 over the frontal thickness of 5–20 cm.

The time-lagged cross-correlations between pairs of sensors were calculated to obtain a second estimate of the mean inclination of thermal and current structures. The mean time-lag corresponding to maximum cross-correlation was used to estimate the apparent effective speed and descent of coherent structures and, as before, to find the inclination from the mean advection speed. The mean was found to be 43° – slightly higher than that of the fronts. The average maximum correlation coefficients (and time lags) at 100 cm vertical separation were 0·47 (11·8 s) for temperature and 0·45 (10·8 s) for currents, and 0·36 (24·2 s), 0·32 (28·0 s) respectively at 200 cm separation. The currents and temperatures measured at the same levels were coherent (coherence > 0·5) for periods exceeding 100 s (equivalent to 6·7 m using a Taylor hypothesis) with near-zero phase. Typical values of the Taylor microscales for current and temperature fluctuations are 1–3 m.

3.2. *The orientation of the thermal fronts*

Figure 4 shows a record obtained with the three-dimensional array (§2.2) spanning the depth interval 4·55–7·05 m. The mean wind speed was 7·8 m s^{-1} and the air temperature was about 2·1 K above the water surface temperature with wet bulb depressed by 2·0 K. Sky was overcast, weather dry. The three plots show the temperatures measured simultaneously by (*a*) six thermistors on the vertical spar; (*b*) three thermistors aligned in the flow direction and (*c*) four thermistors aligned in the horizontal across the flow. (The orientation varied within $\pm 12°$ during the 20 min period whilst the flow direction measured by the small sensing vane varied by $\pm 2·4°$.) The sequential arrival of temperature fronts at the sensors aligned with the flow can be seen in (*b*), especially at about 270, 600 and 870 s. The front at 600 s appears to have a split structure reminiscent of the pattern which might be found during vortex pairing (see Thorpe 1971, figure 5; Browand & Winant 1973, figure 3) or the development of secondary vortices on the sharp interface between neighbouring billows (see Thorpe *et al.* 1977, figure 3 (*c*) near 1400 s). There appears to be little change in the pattern sensed by the three thermistors. The three records and similar ones (a total of 22 in all) have been used to follow the progress of fronts as they pass through the moored array. Figure 5 shows distance–time plots of the arrival of four fronts at sensors spaced vertically, along the flow, or across the flow. As remarked already (§1) the front arrives first at the upper sensor and appears to descend at a fairly uniform speed through the array. The apparent longitudinal advection speed of the fronts, measured from their successive arrival at the sensors aligned with the flow, is fairly uniform, and is within 4 % of the measured mean flow speed (a difference which is not significantly greater than the accuracy of the velocity sensors). The arrival times at the sensors aligned across the flow differ by much less than the others, and no regular pattern is observed, the front sometimes being bowed (figure 5*c*) or kinked (*d*). The mean currents were found to be directed at $19·2 \pm 10·9°$ to the right of the loch axis and the fronts were inclined to the horizontal at $50·8 \pm 11·4°$ (see figure 6). The mean surface defining the front intersects a horizontal plane in a line inclined at $79·9 \pm 17·1°$ to the right of the mean current. The fronts are thus almost normal to the direction of flow and to the wind direction.

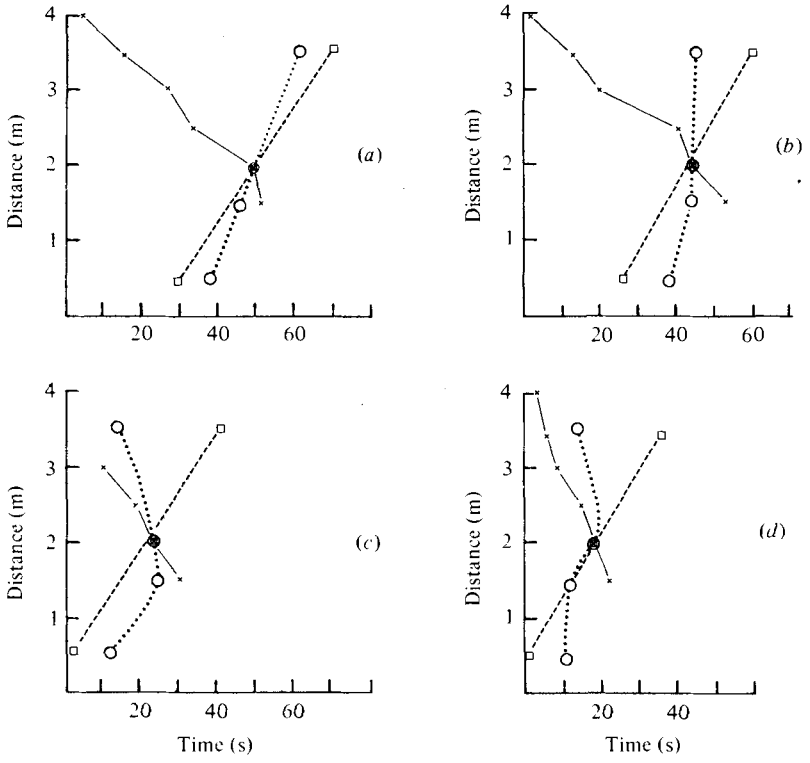

FIGURE 5. Examples of time *versus* distance plots showing the arrival times of four thermal fronts at successive sensors spaced: ×, vertically; □, along the flow; ○, across the flow. They thus define the shape of the fronts. (*a*) $T = 232 \pm 4°$, $V = 0 \pm 5°$; (*b*) $T = 236°$, $V = -6 \pm 3°$; (*c*) $T = 232 \pm 3°$, $V = -7 \pm 3°$; (*d*) $T = 230°$, $V = 0 \pm 4°$ where angles T and V give the true orientation of the tube (the loch axis is along a direction 036°) and the relative orientation of small direction vane respectively.

Some additional information which appears relevant to the structure of the fronts was obtained using the inverted echo sounder (§2.3). Figure 7 shows a typical record obtained with the sounder at 34 m depth. The horizontal co-ordinate is proportional to time (increasing to the left). The level of the surface is marked. The surface itself is not distinctly shown because the surface waves are not resolved in this record. Below the surface are dark 'clouds' of sound-scattering targets, which are bubbles created by breaking waves. The bubbles can be seen to extend down to some 5 m just to the left of the first time mark. Below the surface are two strong horizontal lines, *A* and *B*, which are respectively a streamlined float and second reflexion of the sound between the sonar and a floatation tube *C*. The neutrally buoyant drogued targets are marked by the wavy lines between *B* and *C*. The neighbouring horizontal traces mark the swivels which attach their fishing lines onto the vertical wire.

The five targets are equally spaced between 5 and 15 m and can be seen to vary their depths over periods of 1–10 min. The upper targets have the greater mean displacement, more frequent variations, and sometimes exhibit motions which are uncorrelated with those of the lower targets. In the record arrows mark the traces of

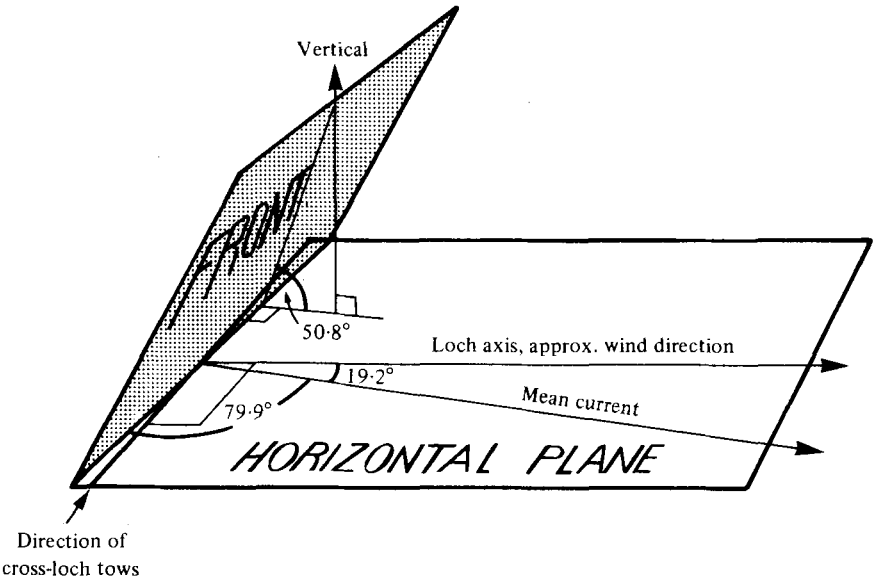

FIGURE 6. Diagram showing the mean orientation of a thermal front.

the upper four targets where they are sequentially displaced downwards, the upper first, just after the first appearance at the surface of the bubbles forming the cloud to which we have already referred. The pattern is indicative of a downward flow, helping to carry the bubbles from the surface, which gradually penetrates to greater depths. The slopes of this, and other similar patterns, have been measured and converted into an inclination to the horizontal using the mean horizontal advection speed measured by the rotor on the nearby three-dimensional array. The mean inclination is $51 \pm 22°$ which, although showing greater variation, is consistent with the inclination of the fronts. The r.m.s. maximum vertical velocities calculated from the vertical displacement of the targets over successive periods of 5 min are 2·0, 2·5, 3·5 and 4·3 cm s^{-1} in mean winds of 4·8, 7·3, 9·1 and 10·5 m s^{-1} respectively. About 60 % of the bubble clouds which persist for several minutes have associated downward vertical motions of the targets as in figure 7. The dynamics of bubbles is thus affected by the large-scale motions in the mixing layer.

The cross-correlations between different sensors on the three-dimensional array were calculated to determine the validity of the Taylor hypothesis and the scales of structures having significant correlations. No significant difference was found between the cross-correlations between sensors spaced along the flow direction and their auto-correlations calculated at time-lags corresponding to the time (e.g. see figure 5) taken for the flow to advect through the distance separating the sensors. In this sense the Taylor hypothesis appears to be valid to scales of 3 m, the maximum extent of the array. Sensors separated by more than 1 m in the flow direction were better correlated than those which were separated by the same distance vertically (see also Thorpe & Hall 1977), and the latter better correlated than were sensors placed across the flow. A correlation of 0·5 was found at effective sensor spacings of approximately 1·53, 1·42 and 1·30 m at 6·5 m depth in the along-flow, vertical and across-flow directions respectively. The mean separation between fronts using the

Taylor hypothesis was approximately 25 m. (For comparison Antonia *et al.* (1979) obtained a correlation coefficient of 0·5 between temperatures measured at points separated by 6 m across the wind direction in measurements at 10·5 m in the atmospheric boundary layer over water when ramps had a mean separation of 17 m.)

3.3. *Skewness of the horizontal temperature derivatives*

The presence of ramps in the temperature signal is reflected in a skewness in the temperature derivatives. Gibson, Friehe & McConnell (1977) noticed that, in laboratory and atmospheric boundary-layer flows, the sign of the skewness of the streamwise temperature gradient, sgn $S(\partial T/\partial x)$, is given by sgn $(\hat{\mathbf{x}}.(\nabla T \times \boldsymbol{\omega}))$, where $\hat{\mathbf{x}}$ is a unit vector in the flow direction, ∇T is the gradient of the mean temperature, and $\boldsymbol{\omega}$ the vorticity of the mean flow. For the conditions in Loch Ness where the mean temperature and speed increase upwards, we should therefore expect that sgn $S(\partial T/\partial x)$ will be negative.

The skewness $S(\partial T/\partial x)$ has been calculated from the temperature measurements made from the moored and towed arrays, converting the moored array data using the Taylor hypothesis. We find the following averaged values:

for moored arrays	$-0{\cdot}685 \pm 0{\cdot}265$ (depths 4·0–8·5 m);
for arrays towed downwind	$-0{\cdot}644 \pm 0{\cdot}115$ (depths 1·8–7·2 m);
for arrays towed upwind	$-0{\cdot}797 \pm 0{\cdot}212$ (depths, 1·9–7·4 m).

Here x is taken in the flow direction, which was always approximately the wind direction. The ramp-like structures in temperature observed from the moored arrays (e.g. figure 1) were reproduced in towed measurements made upwind but, as might be expected for tows at speeds exceeding the flow speed, their sign reversed for downwind tows, so that sudden decreases in temperature marked the fronts. The observed magnitude of $S(\partial T/\partial x)$ agrees well with those in the atmosphere boundary layer quoted by Sreenivasan & Antonia (1977).

It might be expected that, by symmetry, skewness of the cross-loch temperature gradient should be zero. For technical reasons the cross-loch tows were always made in a direction to the left of the wind (i.e. to the N.W. in S.W. winds). The analysis of the cross-loch runs was complicated by the presence of fronts associated with the general circulation of the loch, which extended for several kilometres almost parallel to the shores of the loch. These were often marked on the loch surface by well-defined foam lines (occasionally two or three closely spaced) which persisted for many hours, unlike the wind rows, which were more transitory. Analyses of the records were made by selecting parts which were clear of these fronts of large-scale trends in temperature and, for the cross-loch runs, this sometimes resulted in data sets of less than ideal length.

The mean cross-wind temperature gradient skewness, $S(\partial T/\partial y)$, was $0{\cdot}357 \pm 0{\cdot}347$ (depth range 1·8–8·2 m). This is smaller than the skewness in the wind direction, but much larger than the values found in a turbulent boundary layer by Sreenivasan & Antonia. It should be noticed, however, that since the fronts intersect the horizontal in a mean angle which is inclined at 99·1° to the right of the loch axis (see figure 6) a small positive skewness in the cross-loch tows is expected if the ramps contribute significantly.

3.4. *Spectra*

No attempt was made to remove the effects of surface waves or sensor vibration (§2.1) from the data before analysis, but spectra in which the effects were apparent were rejected.

The temperature frequency spectra measured by the fixed arrays consistently exhibited a slope near $-\frac{5}{3}$ in the frequency range 2×10^{-3} to 0·1 Hz (the Brunt–Väisälä frequency is lower, typically 8×10^{-4} Hz) corresponding to a wavenumber range of about 2×10^{-2} to 2·0 cycles per metre in contrast to the slope near -2 observed in the loch thermocline in the frequency range 0·02 cycles per hour to the Brunt–Väisälä frequency (Thorpe 1977). The temperature wavenumber spectra measured from tows across or along the wind direction (§2.4) were not significantly different, both exhibiting a $-\frac{5}{3}$ slope for wavenumbers greater than about 0·02 cycles per metre (as for the fixed moorings). The spectral slope is consistent with those observed in the atmosphere boundary layer (e.g. Kaimal *et al.* 1972). The coherences between pairs of sensors were also calculated and found not to be significantly different for tows across or along the wind. Typically, for sensors separated by 1·2 m in the vertical, only wavenumbers less than 0·1 cycles per metre have coherence exceeding 0·5.

The frequency spectra of the horizontal currents measured from the moored array in the mixing layer also have slopes close to $-\frac{5}{3}$ in the same frequency range as the temperature spectra. Using the mean observation depth, mean current and the wind stress (estimated from the measured wind speed corrected to 10 m and a drag coefficient of $1{\cdot}3 \times 10^{-3}$) to non-dimensionalize the spectra, we find that they are close to, but slightly below, those of Bradshaw (1967) and very similar to those measured in the Lake of the Woods (Jones & Kenney 1977). The spectra have been used to estimate the ratio of dissipation of turbulent kinetic energy per unit mass, ϵ, on the supposition that the spectra are given by Kolmogorov's expression,

$$E_u(k) = c_0 \epsilon^{\frac{2}{3}} k^{-\frac{5}{3}},$$

appropriate to the inertial subrange, where c_0 is a constant here taken as 0·47 (Heathershaw 1979). At mean wind speeds of 4·5 (and 7·9) m s^{-1} we find that ϵ is equal to $2{\cdot}8 \times 10^{-8}$ ($1{\cdot}26 \times 10^{-7}$) m^2 s^{-3} in the depth ranges 4–7 (6–7) m.† These are reasonably consistent with estimates of Dillon & Powell (1976, 1979) in Lake Tahoe, and with the assumption of an inertial subrange if we accept

$$k_0 = c_1 \epsilon^{-\frac{1}{2}} N^{\frac{3}{2}}$$

for the wavenumber of the outer end of an inertial subrange limited by buoyancy (see for example Weinstock 1978, where c_1 is of order unity).

† These compare with estimates of $N^2 d^3$ of $1{\cdot}6 \times 10^{-8}$ (and $4{\cdot}8 \times 10^{-8}$) m^2 s^{-3}, where N is the mean Brunt–Väisälä frequency and d is the r.m.s. displacement (Thorpe 1977) found from the P.C.M. profiles, which thus appear to underestimate ϵ by a factor of about 2.

4. Discussion

It is tempting to seek a similarity between the temperature fronts or ramps in the loch and the structures found in the boundary layers of the atmosphere or in laboratory experiments. Acknowledging the similarity of the scaled spectra, it might be expected that corresponding structures should be found in the atmospheric boundary layer. The mean angle of inclination of the fronts reported in §3.2 are indeed close to those measured in an unstably stratified boundary layer over water by Antonia *et al.* (1979). The agreement is, however, perhaps slightly fortuitous (but see later) since Phong-annant *et al.* (1980), reporting ramps in both stable and unstable conditions over land, find that the inclination increases with height above the boundary, and the appropriate scaling is not clear. Indeed the smaller inclinations found in §3.1 suggest that significant variation of mean slopes does occur. The atmospheric fronts advect at speeds close to that of the mean wind and are accompanied by ramps in the velocity of the same sense as those in the loch (e.g. in an unstable, hot-earth, boundary layer the temperature ramps mark the arrival of cold, more rapidly moving, air descending from higher levels). Information about the cross-flow structure of the fronts is lacking, and the variations shown in figure 5 give little clue to the full extent of fronts in the loch except that it exceeds 3 m.

It seems probable that the ramps are associated with boundary-layer turbulence at heights (or depths) less than the Monin–Obukov length scale where the dynamic effects of buoyancy are, on the whole, negligible and the temperature field – distorted by a mechanism not unlike frontogenesis in the atmosphere – is, for the most part, a passive marker. In some regions however, in particular in the fronts themselves, where the gradient Richardson number was found to be small (§3.1) but not insignificantly so, buoyancy may be important.

In this connexion, it is interesting to examine the similarity to laboratory flows, in particular the experiments of Chen & Blackwelder (1978) who introduced temperature as a marker by slightly heating the upper wall of a wind tunnel (comparisons with other authors have been made extensively by, for example, Antonia *et al.*). The development of temperature ramps in the outer region of the boundary layer was observed and the slope of the fronts increased away from the wall reaching about 45° at distances of $0{\cdot}45\delta$, where δ is the boundary-layer thickness, the distance from the wall at which the velocity is equal to $0{\cdot}99u_\infty$, where u_∞ is the free-stream velocity. Our measurements showing similar tilts are at comparable depths if, for δ, we take the thickness of the mixing layer. The velocity fields near the front are consistent with those found in the loch, and the value of the velocity–temperature cross-correlation coefficients found by Chen & Blackwelder to be 0·61 over much of the boundary layer, are similar to that reported in §3.1 if one accounts for the change in sign by noting that in the laboratory the velocity increases away from the upper boundary. It is tempting also to compare values of $F\delta/u_\infty$, where F is the mean frequency of the arrival of fronts at a fixed position. Chen & Blackwelder find a value near 0·37 over much of the layer, whilst (interpreting δ as before) we find values ranging from 0·33 to 0·63. The presence of surface waves, the absence of a layer corresponding to a viscous sublayer, the imprecise definition of boundary-layer thickness and the presence of an underlying thermocline in the loch, makes exact comparison and scaling uncertain.

Some caution is needed in applying the results to the open ocean, where the larger fetch and scale allows the full development of Ekman layers, swell to propagate from distant storms and large wind waves to develop. The general circulation pattern of the loch, and the observed turning of the current to the right of the wind (§3.2) suggest that even there the effect of the Earth's rotation cannot be neglected and that the upper layer has an Ekman-like structure. To what extent waves affect the mixing-layer dynamics is not known, although Stewart & Grant (1962) were led to infer that almost all wave dissipation is concentrated essentially above the trough line and that 'splash' turbulence penetrates very little into the body of the fluid.

Other than the obvious lines of foam which were present during many of the experiments and in particular during the tows across the wind direction, clear signals which can be associated with wind rows have proved elusive. Attempts to define a mean thermal structure below wind rows by analysis of the cross-wind tows, or to recognize a pattern as a wind row passes over the moored three-dimensional array, have proved inconclusive. Further studies are planned.

5. Conclusions

We have identified large-scale coherent structures in the turbulent mixing layer of a freshwater lake. Observations from several sensors show the presence of downward-moving warm water of near-surface origin with greater than average horizontal velocity separated by narrow tilted interfaces, fronts, from slower moving, colder water.

The presence of vertical motions associated with warm water do not of course imply that a vertical transfer of heat accompanies the process. Internal waves have the same pattern but may transfer no heat at all. The presence of frequent inversions in the vertical temperature profiles in the region between the fronts is, however, indicative of turbulent diffusion, though on a scale generally smaller than the vertical extent of the fronts themselves. Isotropy in the temperature field is found on scales of one metre or less. Judging by the measured values of the local Richardson numbers the fronts themselves seem to be only marginally unstable, if unstable at all, and it is not clear whether the descent of fluid of increased speed (such as that which follows a front) towards the thermocline will, or will not, so increase the shear that the thermocline will become locally unstable. It is tempting to suppose that the temperature 'bursts' reported by Dillon & Caldwell (1978) at the foot of the mixing layer may be due to instability caused by enhanced shear accompanying the arrival of fluid from near the sea surface. The secondary mechanism of internal wave generation by the descending fluid, and subsequent internal wave breaking at the top of a thermocline across which there is shear (Thorpe 1978*b*), is an alternative mechanism which cannot yet be excluded.

More careful observations of the ocean mixing layer are needed. What is clear is that in many respects the mixing layer is similar to the near-surface atmospheric boundary layer.

It is a pleasure to acknowledge the help of Messrs M. Bray, P. N. Humphries and D. Harfield in the experiments at Loch Ness and the kind hospitality and numerous flasks of coffee supplied by Mrs M. MacLennon of Lewiston, Drumnadrochit.

REFERENCES

ANTONIA, R. A., CHAMBERS, A. J., FRIEHE, C. A. & VAN ATTA, C. W. 1979 Temperature ramps in the atmospheric surface layer. *J. Atmos. Sci.* **36**, 99–108.

BRADSHAW, P. 1967 Inactive motion and pressure fluctuations in turbulent boundary layers. *J. Fluid Mech.* **30**, 241–258.

BROWAND, F. K. & WINANT, C. D. 1973 Laboratory observations of shear-layer instability in a stratified fluid. *Boundary-layer Met.* **5**, 67–78.

CHEN, C. H. P. & BLACKWELDER, R. F. 1978 Large-scale motion in a turbulent boundary layer: a study using temperature contamination. *J. Fluid Mech.* **89**, 1–32.

DILLON, T. M. & CALDWELL, D. R. 1978 Catastrophic events in the surface mixed layer. *Nature* **276**, 601–602.

DILLON, T. M. & POWELL, T. M. 1976 Low-frequency turbulence spectra in the mixed layer of Lake Tahoe, California–Nevada. *J. Geophys. Res.* **81**, 6421–6427.

DILLON, T. M. & POWELL, T. M. 1979 Observations of a surface mixed layer. *Deep-Sea Res.* **26**, 915–932.

FALLER, A. J. & CAPONI, E. A. 1978 Laboratory studies of wind-driven Langmuir circulations. *J. Geophys. Res.* **83**, 3617–3633.

GARRETT, C. J. R. 1976 Generation of Langmuir circulations by surface waves – a feedback mechanism. *J. Mar. Res.* **34**, 117–130.

GIBSON, C. H., FRIEHE, C. A. & MCCONNELL, S. O. 1977 Structure of sheared turbulent fields. *Phys. Fluids Suppl.* **20**, 156–167.

HEATHERSHAW, A. D. 1979 The turbulent structure of the bottom boundary layer in a tidal current. *Geophys. J. Roy. Astro. Soc.* **58**, 395–430.

JONES, I. S. & KENNEY, B. C. 1977 The scaling of velocity fluctuations in the surface mixed layer. *J. Geophys. Res.* **82**, 1392–1396.

KAIMAL, J. C., WYNGAARD, J. C., IZUMI, Y. & COTÉ, O. M. 1972 Spectral characteristics of surface-layer turbulence. *Quart. J. Roy. Met. Soc.* **98**, 563–589.

KENNEY, B. C. 1977 An experimental investigation of the fluctuating currents responsible for the generation of windrows. Ph.D. thesis, University of Waterloo.

LABARBERA, M. & VOGEL, S. 1976 An inexpensive thermistor flow meter for aquatic biology. *Limnology & Oceanog.* **21**, 750–756.

LEIBOVICH, S. 1977 On the evolution of the system of wind drift currents and Langmuir circulations in the ocean. Part I. Theory and averaged current. *J. Fluid Mech.* **79**, 715–743.

LEIBOVICH, S. & RADHAKRISHNAN, K. 1977 On the evolution of the system of wind drift currents and Langmuir circulations in the ocean. Part II. Structure of Langmuir vortices. *J. Fluid Mech.* **80**, 481–507.

MURRAY, J. & PULLER, L. 1910 Bathymetrical survey of the Scottish fresh-water lochs during the years 1897–1909. *Report of the Scientific Results*, vols. 1–6. Edinburgh: Challenger Office.

PHONG-ANANT, D., ANTONIA, R. A., CHAMBERS, A. J. & RAJAGOPALAN, S. 1980 Features of the large scale motion in the atmospheric surface layer. (submitted to *J. Geophys. Res.*)

POLLARD, R. T. 1977 Observations and theories of Langmuir circulations and their role in near surface mixing. In *A Voyage of Discovery*, G. Deacon 70th anniversary vol. (ed. M. Angel). Pergamon.

RIEDL, R. J. & MACHAN, R. 1972 Hydrodynamic patterns in the lotic inter-tidal sands and their bioclimatological implications. *Mar. Biol.* **13**, 179–209.

SCOTT, J. T., MYER, G. E., STEWART, R. & WALTHER, E. G. 1969 On the mechanism of Langmuir circulations and their role in epilimnion mixing. *Limnology & Oceanog.* **14**, 493–503.

SREENIVASAN, K. R. & ANTONIA, R. A. 1977 Skewness of temperature derivations in turbulent shear flows. *Phys. Fluids* **20**, 1986–1988.

STEWART, R. W. & GRANT, H. L. 1962 Determination of the rate of dissipation of turbulent energy near the sea surface in the presence of waves. *J. Geophys. Res.* **67**, 3177–3180.

THORPE, S. A. 1971 Experiments on the instability of stratified shear flows: miscible fluids. *J. Fluid Mech.* **46**, 299–319.

THORPE, S. A. 1977 Turbulence and mixing in a Scottish loch. *Phil. Trans. Roy. Soc.* A **286**, 125–181.

THORPE, S. A. 1978*a* The near-surface ocean mixing layer in stable heating conditions. *J. Geophys. Res.* **83**, 2875–2885.

THORPE, S. A. 1978*b* On internal gravity waves in an accelerating shear flow. *J. Fluid Mech.* **88**, 623–639.

THORPE, S. A. & HALL, A. J. 1977 Mixing in upper layer of a lake during heating cycle. *Nature* **265**, 719–722.

THORPE, S. A., HALL, A. J., TAYLOR, C. & ALLEN, J. 1977 Billows in Loch Ness. *Deep-Sea Res.* **24**, 371–379.

THORPE, S. A. & HUMPHRIES, P. N. 1980 Bubbles and breaking waves. *Nature* **283**, 463–465.

THORPE, S. A. & STUBBS, A. R. 1979 Bubbles in a freshwater lake. *Nature* **279**, 403–405.

WEINSTOCK, J. 1978 Vertical turbulent diffusion in a stably stratified fluid. *J. Atmos. Sci.* **35**, 1022–1027.

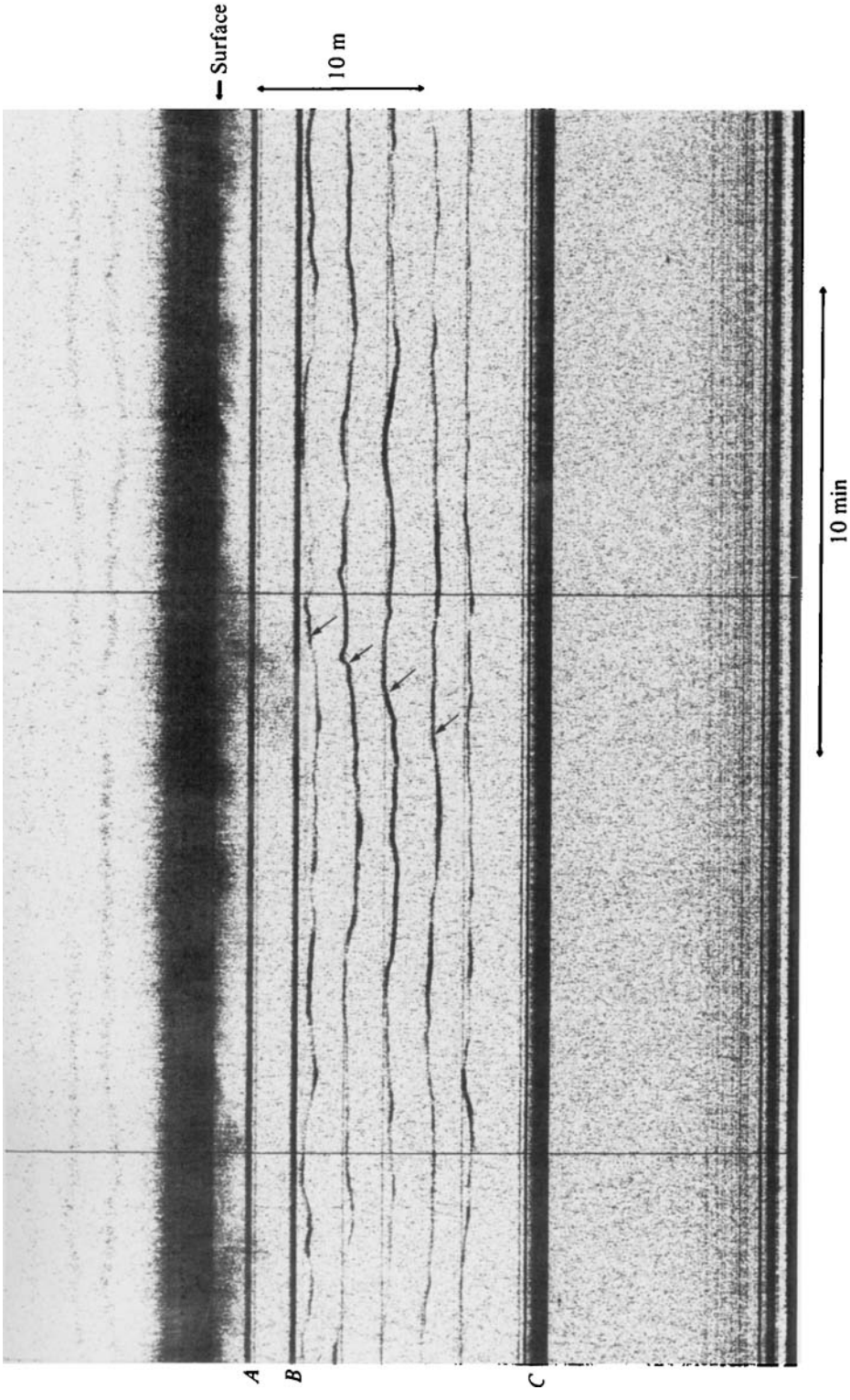

FIGURE. 7. Sonar record of depth *versus* time (increasing to the left) showing the movement of five neutrally buoyant floats (between levels *B* and *C*). Clouds of bubbles can be seen below the surface. The two vertical lines are time marks. See the text (§ 3.2) for an explanation.